*Biochimica et Biophysica Acta* 939 (1988) 509–522
Elsevier



BBA 73769

# Nuclear membrane fusion in electrofused mammalian cells

U. Bertsche [a], A. Mader [b] and U. Zimmermann [b]

[a] *Gesellschaft für Strahlen- und Umweltforschung, Frankfurt / Main,*
*and* [b] *Lehrstuhl für Biotechnologie der Universität Würzburg, Würzburg (F.R.G.)*

(Received 15 May 1987)

Key words: Membrane fusion; Electrofusion; (Muntjac cell); (Ehrlich ascites tumor cell); (V 79-S181 cell)

**Fusion of nuclei was studied in electrofused cells using staining procedures and DNA flow cytometry. Homogeneous and heterogeneous electrofusion of Ehrlich ascites tumor cells. Muntjac cells and V79-S181 cells were performed in balanced-salt solutions at low temperature. Incubation of the cells subjected to electrofusion in fusion media for about 2 h was required to complete cell fusion and, in particular, nuclear membrane fusion. Under optimum electrofusion conditions it was found that fusion of nuclei is a very frequent event. Half of the fused cells (about 30 to 50% of the field-exposed cells) underwent nuclear membrane fusion. It is shown that the high frequency of nuclear membrane fusion in electrofused, unsynchronised cells resulted from intracellular dielectrophoresis occurring during cell alignment. In accordance with theory, maximum nuclear membrane fusion was observed using alignment fields of between 1 and 4 MHz (depending on the cell species), that is above the frequencies at which the plasmalemma capacity no longer shielded the cell interior from participation in the conduction process. In this frequency range a potential difference can be built up across the nuclear membrane leading to repositioning of the nuclei into the contact zone of the plasmalemmas of two attached cells. This intracellular dielectrophoresis apparently facilitated fusion of nuclei once intermingling of the plasma membranes had occurred. It was further demonstrated that exponentially growing cells showed higher cell fusion rates than cells taken from the unfed plateau phase. One, but not the only reason, might be the higher ATP content of exponentially growing cells compared to cells of the plateau phase. Addition of external ATP to plateau phase cells during electrofusion resulted, in accordance with this assumption, in an increase of fusion frequency, whereas ATP had apparently no effect on the fusion yield of exponentially growing cells. G1 cells obtained by mitotic selection after nocodazole-induced blockage in metaphase also showed higher cellular and nuclear membrane fusion yields than exponentially growing cells. Most importantly, it could be demonstrated both experimentally and theoretically that electrofusion of cells in a dielectrophoretically aligned chain is controlled by a simple law of probability resulting predominantly in fusion of two cells independent of the number of cells in the chain. The likelihood of fusion of various numbers of cells in a chain is given by the appropriate power of the probability of two-cell fusion. These experimental and theoretical findings could explain why electrofusion leads to a high number of hybrids despite the fact that cell chains normally consist of more than two cells.**

## Introduction

Electrofusion has been successfully used for somatic hybridisation of bacteria, yeast and plant

Correspondence: U. Zimmermann, Lehrstuhl für Biotechnologie der Universität Würzburg, Röntgenring 11, 8700 Würzburg, F.R.G.

protoplasts as well as of mammalian cells [1–5]. Even though the yield of viable hybrids is very high compared to conventional fusion techniques, a further increase in efficiency is expected if fusion of the nuclei can be enhanced, once fusion of the plasmalemmas of at least two cells has occurred. In chemically or virally induced fusion, nuclear membrane fusion has been reported only seldom and then only after synchronisation by colcemide treatment, by centrifugation [6], or by GTP addition [7].

In contrast Zimmermann et al. [8] reported some evidence that fusion of nuclear membranes occurred some time after electrofusion of the plasmalemma of dielectrophoretically aligned, unsynchronised erythroleukaemic cells.

In addition, Richter et al. [9] observed movement and accumulation of pigments in sea urchin eggs in the contact zone of at least two adhering cells during cell alignment under the influence of an alternating inhomogeneous field. These two observations suggest that the hybrid yield in electrofusion is determined by movement and close approach of the two nuclei of adjacent cells in the contact zone which would undoubtedly facilitate nuclear membrane fusion and subsequently syngamy once the plasmalemma membrane had been electropermeabilised.

We therefore studied in detail the influence of the field parameters on the yield of cellular and nuclear membrane fusion by monitoring fusion by the use of appropriate dyes for staining the nuclei.

The studies were performed on four different (suspension and attaching) cell lines whereby electrofusion were carried out, in contrast, to the usual procedure [1–5,8,9], in balanced-salt solutions at low temperature. These conditions are similar to those successfully used for electric field-mediated protein and gene transfer [10–12].

The data demonstrated that under these conditions fusion of nuclei is a very frequent event provided that appropriate field conditions were used. Half of the fused cells underwent nuclear membrane fusion. The results also showed that electrofusion favoured two-cell and two-nuclei fusion even in very long cell chains, and that the probability of this event was controlled by a simple physical law.

## Materials and Methods

*Cell culture*

The cell lines EAT-F2 (Ehrlich ascites tumour, attaching line), EAT-F1 (suspension line) (both derived from clones of a line given by courtesy of K. Karzel, Bonn, F.R.G.), V 79-S181 (attaching cell line, obtained by courtesy of G. Iliakis, Philadelphia, U.S.A.) and Muntjac (male chromosome constitution, attaching cell line, delivered from Flow Laboratory, Heidelberg, F.R.G.) were grown in exponential culture, unless otherwise stated. EAT-F2 was grown in A4 medium supplemented with 10% calf serum, EAT-F1 in A2 medium supplemented with 20% horse serum, V 79-S181 and Muntjac in MEM and in F10 medium, respectively, both supplemented with 15% foetal calf serum. Whereas EAT and V 79-S181 cell lines showed constant doubling times of 11–12 h and 10 h, respectively, the Muntjac cell cycle was sometimes variable, ranging from about 15 to 30 h.

The attaching cell lines were trypsinized and reincubated for 1 h in prewarmed, fresh nutrition medium before electrofusion.

After harvest and centrifugation the cells were washed in A2BSS solution consisting of 27 mM glucose, 70 mM NaCl, 3.4 mM KCl, 0.6 mM $KH_2PO_4$ and 1.1 mM $Na_2HPO_4$. The cells were resuspended in cold fusion solution consisting of A2BSS plus 0.1 mM calcium acetate and 0.5 mM magnesium acetate [13,14] at a suspension density of about $5 \cdot 10^7$ cells/ml. The pH of this fusion medium was adjusted to 7.3. For fusion between cells of different lines the suspensions were mixed in a ratio of 1 : 1.

*Electrofusion*

For field application the cell suspensions were precooled to 4°C for at least 10 min and then pipetted into the outer jacket of a helical fusion chamber (described in Ref. 13). The distance between the parallel wound wires of the helical chamber was 200 $\mu$m. Although the helical chamber was kept in a 4°C bath during the entire procedure, it should be noted that the actual temperature in the chamber once the alternating field has been applied may rise to about 10°C (Broda and Zimmermann, unpublished data). The elec-

tronic equipment of GCA Corporation developed by Büchner and Arnold, University Würzburg, F.R.G., was used for electrofusion. If not otherwise stated, an alternating field of 220 V/cm strength and 1.7 MHz frequency was applied for 30 s, followed by square field pulses of 5 kV/cm strength and 15 μs duration. Preliminary experiments showed that this duration yielded the highest fusion index. In particular, pulses which lasted longer than about 30 μs were always less effective because of adverse side effects on the membrane and other parts of the cell in the presence of highly conductive solutions [1–5]. The field pulses were applied in two trains each consisting of three pulses. The time interval between the pulses of each train was 0.7 s and the two trains were separated by a time interval of 10 s. After breakdown the alternating field was applied with exponentially decreasing amplitude for a further 200 s. Afterwards, the helical chamber was transferred to a water bath (37 °C) for 10 min followed by gentle centrifugation for 5 min in order to remove the fused and unfused cells from the electrodes. After opening the helical chamber the internal tube around which the electrode wires were wound was carefully removed and the cell pellet in the outer jacket resuspended in 10 ml of the fusion medium for a period (given below) at 37 °C (see below). This incubation period was termed postfusion time.

*Microscopic analysis*

Cells were centrifuged and the pellet was immediately fixed by using Carnoy's fixative (3 parts methanol and 1 part acetic acid). However, Muntjac cells were pretreated in a hypotonic solution (1 part A2BSS and 3 parts distilled water) for 15 min before fixation. The cells were kept in the cold fixative overnight, after which an aliquot of the fixed cells (about 20 μl) was applied to a microslide that had been stored in cold water and had been dried over flame. Staining used a 3% Giemsa solution (consisting of 6.5 parts distilled water, 3.2 parts A2BSS and 0.3 parts Giemsa) for 15 min at room temperature. This procedure was used because Muntjac nuclei appeared more regular after fixation. The stained nuclei were counted and analysed in a light microscope (Zeiss Universal) at 200 × or 520 × magnification. Control experiments indicated that fixation, treatment by hypotonic solutions and the staining process did not change the spatial arrangement of the nuclei within fused cells. In more than 90% of the control experiments the nuclei were found to be located in the center of the cell.

The extent of cell or nucleus fusion was measured by the determination of the cell fusion or nuclear membrane fusion index, respectively. These indices were defined as follows:

$$F_C = \frac{n + n'}{N} = \frac{n}{N} + F_N \tag{1}$$

and

$$F_N = \frac{n'}{N} \tag{2}$$

whereby $n + n' < N$. $F_C$ is the cell fusion index and $F_N = n'/N$ is the nuclear membrane fusion index; $n$ = number of unfused nuclei in fused cells, $n'$ = number of nuclei found in the nuclear fusion process and $N$ = total number of cells counted.

According to the above definition the nuclear membrane fusion index $F_N$ is a component of the cellular fusion index $F_C$.

Exponentially growing cells of all four lines contained about 1 to 2% binucleates probably arising from spontaneous fusion or failure of cytokinesis. However, 5% or more of cells from unfed stationary cultures may be binucleates. In most of the experiments cells were taken from the log-phase, therefore the error of the determinations of the fusion indices introduced by spontaneous fusion can be neglected. A larger error may result from the difficulty in distinguishing cells which are just beginning the fusion process from unfused, adjacent cells. As a rule, only those cells were counted in which the plasmalemmas were partly or completely intermingled (Fig. 1) as reflected by continuous staining along the contact zone.

Fusing nuclei could easily be distinguished from multinucleates by variation of the focal plane of the microscope; under these conditions multinucleates exhibited a clear separation of the nuclei whereas nuclei in the process of fusion showed a common area of adjacent membranes (Fig. 1).

a

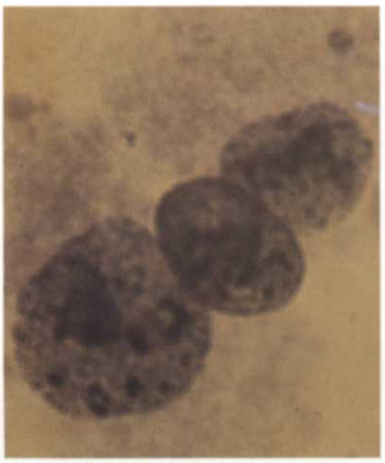

b (left)

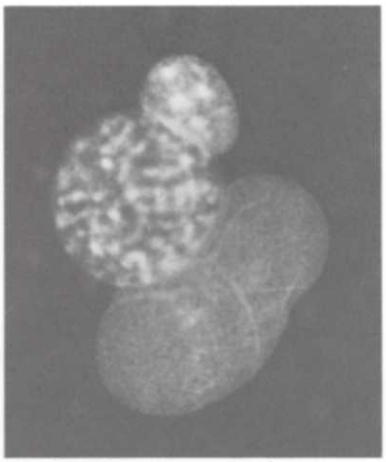

b (right)

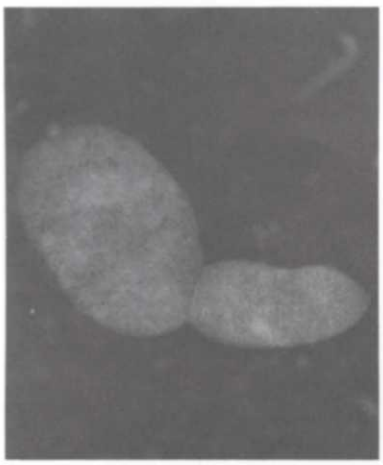

c(left)

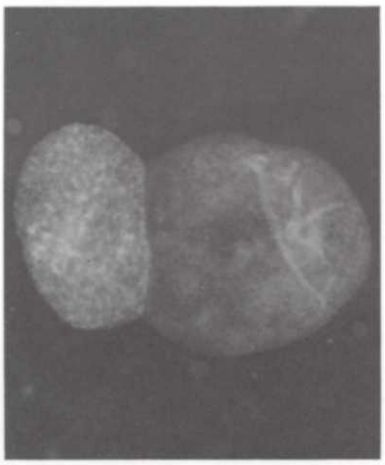

c(right)

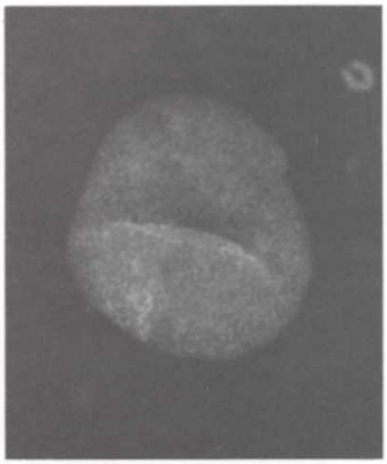

d

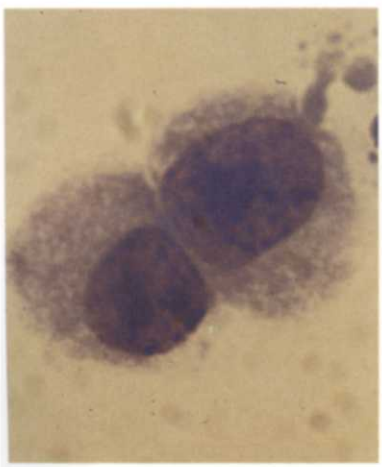

f(left)

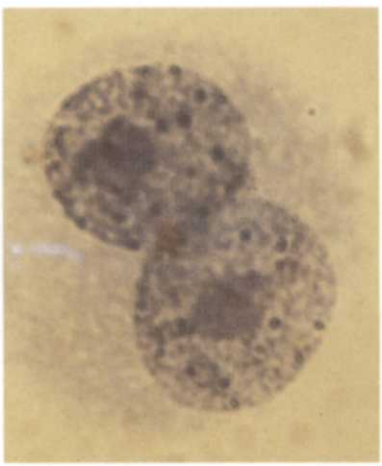

f(right)

g

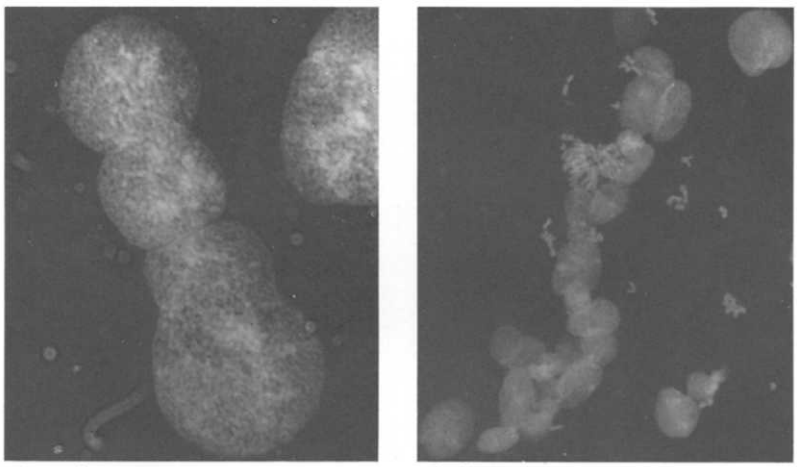


Fig. 1. Successive phases of nuclear membrane and nuclear fusion in mammalian cells subjected to electrofusion (alternating field: 220 V/cm strength and 1.7 MHz frequency for 30 s, followed by 2×3 field pulses of 5 kV/cm strength and 15 μs duration, for further details, see text). Nuclei were Giemsa stained after fixation with Carnoy's fixative (Zeiss microscope, 520× magnification, oil immersion). (a) Orientation of nuclei to the plasmalemma contact zone of two dielectrophoretically adhered cells (EAT-F2 cells, photograph taken after a postfusion time of $t = 0$). (b) Attachment of nuclei of EAT-F2 cells in the contact region (left side: three nuclei, and right side: four nuclei, one of which is in prophase). (c) Enlargement of the nuclear membrane contact zone (left side: EAT-F2 and Muntjac cells, at which Muntjac nuclei often appeared ellipsoid after hypotonic treatment, right side: homogeneous fusion of EAT-F2 cells). (d) Engulfment of nuclei of comparable sizes (EAT-F2 cells, photograph taken after $t = 2$ h). (e) Linear fusion of six (left side) and 20 (right side) nuclei along the cell chains (fusion between EAT-F2 and Muntjac cells). (f) Cell fusion between EAT-F2 cells without reorientation of the nuclei into the contact zone of the plasmalemma (left side: photograph taken during plasmalemma fusion at which the fusion cleft is still partly visible, and right side: binucleate after completion of cell fusion, both nuclei appear as separate entities). (g) Fusion of nuclei of Muntjac (large) and EAT-F2 (small). This photograph clearly shows that fusion of membranes between the two nuclei occurred, indicated by the distribution of the 'light-stained' membrane material from Muntjac over the area of the 'dark-stained' membrane of EAT-F2.

*Flow cytometry*

DNA flow cytometry provides a reliable and objective method for measuring the cell fusion index, since fused cells contain at least twice the DNA content of their single parentals. Therefore, single staining of cells with ethidium bromide (which stains the nucleus only after removal of RNA) was performed. A sample of about $1 \cdot 10^6$ cells was withdrawn from each probe at various times after electropermeabilisation and treated with a solution containing RNAase, ethidium bromide (25 μg/ml) and Nonidet (0.3 ml/l) to permeabilise the entire plasma membrane [15]. The sample was measured after at least 30 min of incubation in this solution at room temperature, using a modified Ortho Instrument System (Cytofluorometer 30 L) and an argon laser (operating at 300–1000 mW). The DNA histograms (Fig. 2) obtained from control suspensions (without electropermeabilisation, given the subscript '0' in quantities) and suspensions with electrofused cells were analysed for the relative contribution of cells in $G_1$ phase ($T_1$), S phase ($T_2$), $G_2 + M$ phases ($T_3$) and beyond $G_2 + M$ phases ($T_4$). The counts with DNA larger than $G_2 + M$ were separated in regions according to the DNA content: ($T_4$) with content larger than $2C$ but smaller than or equal to $3C$, ($T_5$) between $3C$ and $4C$, etc. The fusion index determined results then from the relative changes in counts in ($T_1$), ($T_4$), ($T_5$), etc. with respect to the control histogram ($T_{1,0}$, $T_{4,0}$, $T_{5,0}$, etc).

$$F = 1 \cdot (T_{1,0} - T_1) + 2 \cdot (T_4 - T_{4,0}) + 3 \cdot (T_5 - T_{5,0}) + \ldots \quad (3a)$$

$$= (T_{1,0} - T_1) + \sum_{n=2}^{k} n \cdot (T_{n+2} - T_{n+2,0}) \quad (3b)$$

The first term in Eqn. 3b, $(T_{1,0}) - (T_1)$, reflects the contribution of $G_1$-phase cells for all fusions irre-

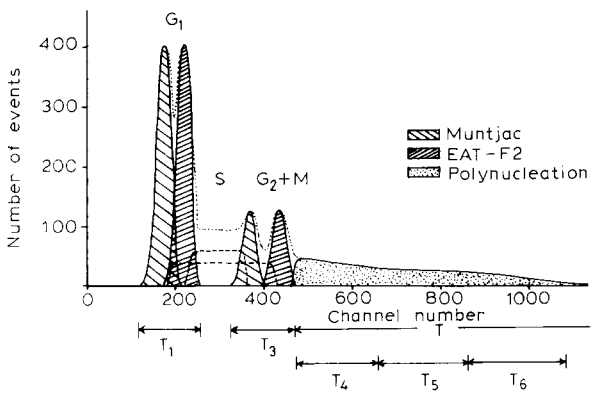


Fig. 2. Schematic drawing of DNA histograms obtained by flow cytometry of two cell lines differing in their DNA content and subjected to electrofusion. Separation of the $G_1$ peaks and $G_2 + M$ peaks of each cell line is possible, if the $G_1$ DNA content differs by more than about 10% from the $G_2 + M$, whereas S phase cells show the usual distribution (dashed lines) and add to each other (dotted line). Fused cells appear in the region denoted by 'T' and are separated according to DNA content in multiples of the $G_1$ content ($1C$) by the regions $T_4$ (DNA content between $2C$ and $3C$), $T_5$ (between $3C$ and $4C$), etc. Measurement of the cell fusion index is thus possible when the relative difference in $G_1$ (region $T_1$) and region T with respect to the control histogram are calculated.

spective of the number of cells involved in the fusion product. The second term, a sum over $n$ (which in principle could be very large, but in practice breaks off at $n = 7$ because more than seven cells are seldom involved, see below) reflects the contribution of each region, $(T_4)$, $(T_5)$, etc. with DNA content larger than $2C$ to the fusion index. A good approximation to Eqn. 3 is given by:

$$F = d_1 + 2 \cdot d_T \tag{4}$$

with $d_1 = (T_{1,0}) - (T_1)$ and $d_T = (T) - (T_0)$, the relative difference in events with DNA content larger than $2C$ (i.e. beyond the $G_2 + M$ peak).

Using this procedure for histogram analysis, the uncertainty estimated in the calculation of $F$ was about $\pm$ (8–12)% and thus not larger than the error resulting from microscopic analysis.

*Particle analyser measurements*

The volume distribution of the cells were measured with a hydrodynamically focussing particle analyser (AEG, Telefunken, Model TF, F.R.G.) as described previously [16]. The orifice dimensions were 100 $\mu$m in length and diameter. The current was adjusted to 0.4 mA (gain 20). For measurements the cells were suspended in A2BSS medium (conductivity 11.6 mS/cm).

## Results

*Morphology of nuclear membrane fusion*

Photographs (Fig. 1) of Giemsa stained cells taken after application of the breakdown pulse illustrate the events involved in nuclear membrane fusion: (I) cell contact associated with flattening of the adjacent plasmalemma regions and simultaneous repositioning of the nuclei into the polar (i.e. membrane contact) regions; (II) attachment of the nuclei; (III) enlargement of the contact region between the attached nuclei and (IV) 'engulfment' of the smaller nucleus by the larger one. No examples of nearly complete fusion events are shown in Fig. 1 because completely fused nuclei could only be distinguished from unfused nuclei by some irregularities in the shape and chromatin staining. In general, phases (I) and (II) can be most easily observed in Giemsa stained samples, whereas phases (III) and (IV) require careful examination at higher magnification (520 $\times$ ).

Occasionally fusion of several nuclei within long chains of cells (about 20 cells spanning the 200 $\mu$m electrode gap) and also fusion of nuclei originating from cells of adjacent chains, was observed. Clearly, intracellular, field-induced movement of nuclei in long fusing cell chains is a rare event (see below).

These studies indicated that complete nuclear membrane fusion took place within at least two hours provided that a large nucleus fused with a smaller one. However, in other cases nuclear membrane fusion might proceed very slowly after phase (II) and might be complete only after several hours.

*Field parameters*

In contrast to electrofusion in weakly-conductive solutions [1–5,13,14] fusion in balanced-salt solutions requires very precise adjustment of the field strength of the breakdown pulse because of the high current density in the field-permeabilised areas of the membrane [4]. Fig. 3 shows the typical

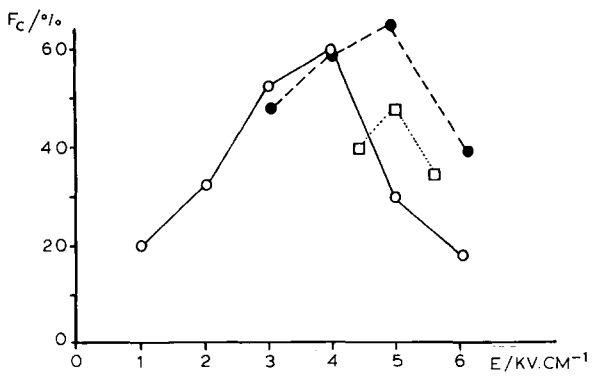


Fig. 3. Cell fusion index (plasmalemma fusion) of various homogeneous mammalian cell systems as a function of the field strength of the fusion pulse (field conditions otherwise as described in Fig. 1): open circles, V 79-S181; closed circles, EAT-F1 cells; open squares, Muntjac cells.

dependence of the cell fusion index on field strength for cells of EAT-F1, Muntjac and V 79-S181. Cells were aligned in an alternating field of 220 V/cm amplitude and 1.7 MHz frequency. Homologous cell fusion was triggered by injection of two trains of three pulses of 15 $\mu$s duration as described above. The fusion indices were determined after 2 h postfusion incubation.

It is evident that a fairly narrow range of field strengths existed in which maximum fusion occurred. However, the cell fusion index never exceeded 50% to 70% (depending on the cell line used). The reasons for this result may be that (1) not all of the cells could be aligned between the electrodes because of the dead volume of the helical chamber [13] and (2) that the field strength was not optimal for both very small and large cells [5,17,18]. Size distribution measurements demonstrated that the size distributions of the three exponentially growing cell lines were relatively broad (not shown).

Because of the radius-dependence of the breakdown voltage it cannot be expected that for different size cells the applied field strength is optimum [5,17,18]:

$$V = 1.5 \cdot a \cdot E \cdot \cos \nu \qquad (5)$$

whereby $V$ = generated membrane potential, $a$ = radius of the spherical cell, $E$ = field strength of the pulse and $\nu$ = the angle between a given membrane site and the direction of the field vector (for discussion, see Ref. 4).

Eqn. 5 holds for the steady state which is reached by use of pulses of 15 $\mu$s duration because the relaxation time of the charging process of the membranes in electrolyte solutions is about 500 ns (Ref. 4, see also below). Eqn. 5 explains that the maximum value of the fusion index should be obtained at slightly higher field strengths for Muntjac and V 79-S181 cells (about 5 kV/cm) compared to a value of 4 kV/cm for EAT-F2 cells which have a 10 to 20% larger radius than that of the other two cell types.

Table I shows that under optimum field strength conditions the nuclear membrane fusion index for EAT-F2 cells reached $37 \pm 2$%, i.e. about half of the value of the cell fusion index. Similar results were obtained (see also below) for heterogeneous fusion (EAT-F2 with Muntjac cells and EAT-F2 with V 79-S181 cells). In this context, it is interesting to note that single trains of 3 or 6 pulses of 15 $\mu$s duration resulted in a decrease of the yield compared to that obtained with two trains of 3 pulses. Table I also presents the nuclear membrane fusion index of homogeneous fusion of EAT-F2 cells for different pulse pattern regimes.

The frequency of the alignment field also had an influence on the cell and nuclear membrane fusion indices. Fig. 4 shows measurements of homogeneous fusion of EAT-F2 and Muntjac cells as a function of the alignment frequency. It is evident that both the cell and nuclear membrane fusion indices of EAT-F2 cells had a maximum value at 1 to 2 MHz and decreased towards higher

TABLE I

NUCLEAR MEMBRANE FUSION INDICES ($F_N$ IN %) OF HOMOGENEOUS AND HETEROGENEOUS CELL SYSTEMS

| Pulse pattern | $F_N$ (%); cell system | | |
|---|---|---|---|
| | EAT-F2/ EAT-F2 | EAT-F2/ Muntjac | EAT-F2/ V79-S181 |
| Control | $7 \pm 1.5$ [a] | $4 \pm 1.5$ | $3 \pm 1.0$ |
| 2×3 | $37 \pm 2.0$ | $26 \pm 4.2$ | $27 \pm 3.2$ |
| 1×3 | $23 \pm 1.3$ | - | - |
| 1×6 | $27 \pm 1.4$ | - | - |

[a] Uncertainties indicate maximum spread of data obtained in different experiments.

frequencies in the same manner. A similar behaviour was observed for fusion of Muntjac cells with the exception that the maximum of two fusion indices occurred between 3 and 4 MHz. Analysis of the photographs indicated that at the optimum frequencies accumulation and attachment of the nuclei of adjacent cells in a chain assumed the maximum value. The 'repositioning' of the nuclei into the contact (fusion) zone was induced by the alternating field, and not by the subsequent breakdown pulse. This conclusion could be drawn from experiments in which cells were subjected to dielectrophoresis leading to membrane contact, without subsequent fusion.

*Postfusion time*

In the following the influence of the postfusion time on the cell and nuclear membrane fusion indices were investigated (Fig. 5). Fusion between cells of exponentially growing EAT-F2 and Muntjac cells was studied. The data confirmed the conclusions from Fig. 1 that 1 to 2 h postfusion incubation was required to complete cell and nuclear membrane fusion. The figure also demonstrates that increase of the alignment frequency from 1.7 MHz to 5 MHz resulted in a decrease of the absolute values of the two indices. However, it is interesting to note that the nuclear membrane

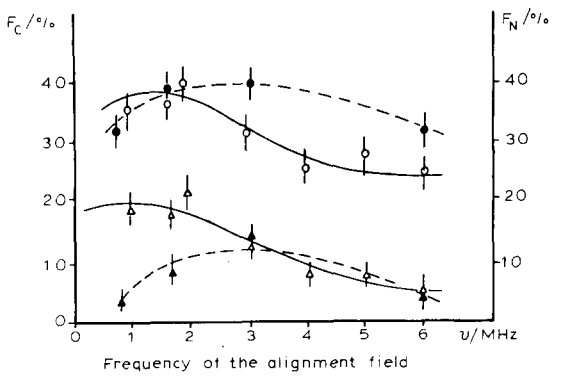


Fig. 4. Fusion indices as a function of the frequency of the alignment field (field conditions otherwise as described in Fig. 1). Circles, cell fusion index; triangles, nuclear membrane fusion index. The open symbols refer to fusion between EAT-F2 cells and the closed symbols to fusion between Muntjac cells. Error bars represent the maximum spread of data obtained in two runs of completely separate experiments made with different batches of cells over a period of approximately six months.

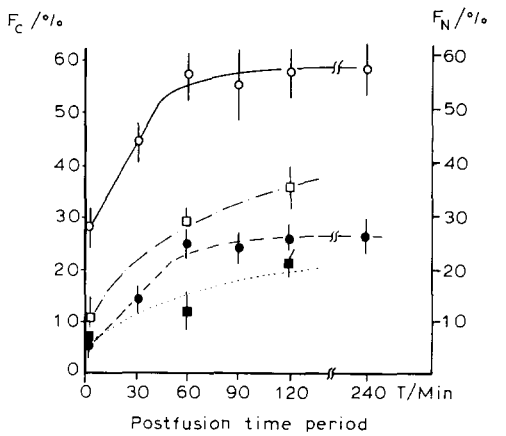


Fig. 5. Fusion indices in dependence on the postfusion period at two different alignment frequencies for the heterogeneous cell system EAT-F2/Muntjac (field conditions otherwise as described in Fig. 1). Open symbols, cell fusion index; closed symbols, nuclear membrane fusion index. Alignment frequencies: circles, 1.7 MHz; squares, 5 MHz. Error bars represent the maximum spread of data obtained in two runs of separate experiments made with different batches of cells over a period of approximately six months.

fusion index in relation to the cell fusion index is higher at 5 MHz than at 1.7 MHz.

In Fig. 6 the fusion indices were determined both microscopically by Giemsa staining of the nuclei and by flow cytometry using ethidium bromide staining of the DNA. Comparison of the curves in Fig. 6 indicate that a parameter somewhat in between the microscopically determined cell and nuclear membrane fusion indices was analysed by use of this technique. A possible cause of this discrepancy could be the nonidet treatment used to permeabilise the plasmalemma before staining. This may affect the results as follows.

If the plasma membranes of cells adhered to each other begin to intermingle in the contact zone at a few sites, they may be rather susceptible to Nonidet influence; in consequence, in this early state of fusion the junctions between the fusing cells may break off during preparation for flow cytometry. However, after prolonged postfusion incubation plasmamembrane fusion occurs over the entire surface in the contact zone. At this stage Nonidet should be unable to separate the fusing cells. Thus, flow cytometry is expected to measure lower fusion indices at the beginning of the post-

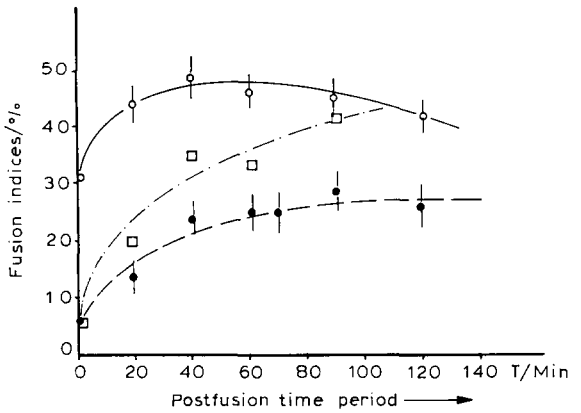


Fig. 6. Fusion indices measured either by microscopic analysis of Giemsa stained cells (open circles, cell fusion index; closed circles, nuclear membrane fusion index) or by flow cytometric DNA determination (open squares, cell fusion index) for the heterogeneous cell system EAT-F2/Muntjac. Field conditions were as described in Fig. 1. Error bars represent the maximum spread of data obtained in two runs of separate experiments made with different batches of cells over a period of approximately six months.

fusion period, whereas after 1 to 2 hours (when cell fusion is completed) the index determined by flow cytometry should be in accordance with the microscopically measured cell fusion index.

From these considerations we conclude that the simple procedure of microscopic analysis of stained cells is more appropriate for studies of this kind than flow cytometry.

It is also interesting to note that the nuclear membrane fusion index of the Muntjac/EAT-F2 system assumed about half of the value of the cell fusion (Figs. 5 and 6 and see above) even though the absolute values of both indices were slightly smaller than those of the homologous cell system. Control experiments showed that spontaneous nuclear membrane fusion occurred at a rate of $6 \pm 3\%$, which is not unusual for untreated cells at the high suspension density of $5 \cdot 10^7$ cells/ml used here. The apparent decline of the cell fusion index at later postfusion times (Fig. 6, open circles) may be caused by a small subpopulation of fusing cells which separated during the preparation for light microscopy.

*Biological parameters*

There is some evidence in the literature that culture conditions and growth cycle can influence cell fusion yield [19]. Cells harvested from the log-phase (45% $G_1$, 35% S and 20% $G_2 + M$) exhibited a dependence of the cell fusion index on the postfusion time as shown in Fig. 7. In contrast, if cells were taken from unfed plateau-phase cultures and fused under the same field conditions almost no fusion was observed. The lack of fusion between cells of the plateau phase cannot be exclusively explained by changes in the modal volume of the size distribution (according to Eqn. 5), since these values only differed by 15 to 25%. It is more likely that the low ATP-content of plateau-phase cells (a factor of about 2 to 3 lower than for exponentially growing cells) is responsible for the absence of fusion. Fig. 7 also represents experiments in which ATP was added to the external medium. In cells taken from the unfed plateau phase, ATP delivered through the permeabilised membranes after pulse application was able to significantly increase the cell fusion index from about 5% to 10%. Because all values were a factor of 2 larger than the control values, this effect can be regarded as statistically significant. However, the high values obtained for exponentially growing cells could not be reached. This was probably due to the low permeability of the membrane to ATP so that the same level of intracellular ATP is not

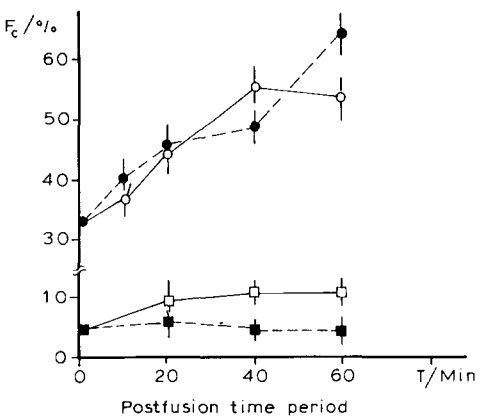


Fig. 7. Cell fusion index as a function of the postfusion period of the homogeneous cell system EAT-F2 in the absence or presence of external ATP. Circles, exponentially-growing cells; squares, plateau-phase cells; closed symbols, no ATP added; open symbols, 0.6 mmol/l ATP added. Field conditions were used as described in Fig. 1. The error bars were estimated from different samples of cells treated under the same experimental conditions during one day.

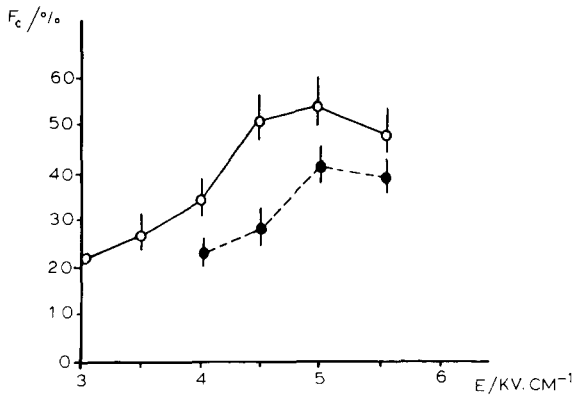


Fig. 8. Cell fusion index of the homogeneous cell system V 79-S181 as a function of the field strength of the fusion pulse (field conditions otherwise as described in Fig. 1). Open circles, $G_1$ cells; closed circles, exponentially growing cells.

reached in the plateau-phase cells compared to the exponential growing cells. Fig. 7 also shows that ATP has apparently no effect on the fusion yield of exponentially growing cells.

Apart from the energy state of the cells, the phase of the cell cycle should influence cellular and nuclear indices. As shown in Fig. 8 $G_1$ cells of V 79-S181 obtained by mitotic selection after nocodazole-induced blockage in metaphase showed higher cellular fusion yields over the whole field strength range compared to exponentially growing cells (consisting mainly of $G_1$, $G_2$, and S cells). This may be explained by the increase in cell radius during the cell cycle (Eqn. 2). Calculations show, however, that the radius-dependence of the generated membrane potential can only account for about 50% of the observed increase in the nuclear fusion index at field strengths below 5 kV/cm. Other factors, e.g. facilitation of the intracellular dielectrophoretic mobility of the nuclei in the $G_1$ phase, may also be important.

*Two-cell versus multiple-cell fusion*

Even though dielectrophoretically aligned cell chains usually contained more than 15 to 20 cells, fusion products from more than two cells were only sometimes observed as mentioned above. In order to arrive at a quantitative description of the likelihood of multiple fusions we measured the partial fusion index, $F_n$. $F_n$ is defined as the ratio of the number of cells containing $n$ nuclei to the total number of cells.

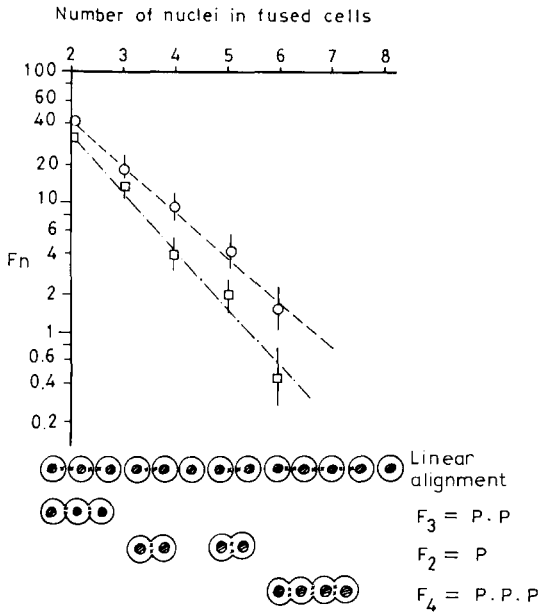


Fig. 9. The partial fusion index $F_n$ ($n = 2, 3, \ldots$) of heterogeneous cells systems analysed after Giemsa staining of the cells. Circles, fusion between V 79-S181 and EAT-F2 cells; squares, fusion between EAT-F2 and Muntjac cells. Broken lines through measured points represent a fit to Eqn. 6. The lower part shows a graphic representation of the probability of fusion between different numbers of cells within a chain according to Eqn. 6: the partial fusion index $F_3$ is the product of $P \cdot P$ with $P$ = probability for fusion of two neighbouring cells in a chain aligned by dielectrophoresis; correspondingly, $F_4 = P^3$ is the probability of fusion of four cells.

According to this definition $F_2$ represents a measure of two-cell fusion, $F_3$ of three-cell fusion and so on. $F_n$ (with $n = 2, 3, \ldots, 6$) was determined microscopically on a large number of Giemsa stained cells as shown in Fig. 9. If the $F_n$ values were plotted versus the number of the nuclei, $n$, in a semilogarithmic plot, straight lines were obtained for the investigated cells systems, EAT-Muntjac and V 79-EAT (Fig. 9). Exponential curves are expected if we assume that (1) breakdown only occurs in the polar region (i.e. the contact zone) of adhered cells in a chain and (2) that the probability, $P$, for fusion of a cell pair after application of the breakdown pulse is constant over the entire chain, i.e. $P < 1 = \text{constant}$. According to Eqn. 5 the first assumption seems to be reasonably fulfilled at low cell suspension densities at which cell chains were separated from each other in the electrode gap. The second as-

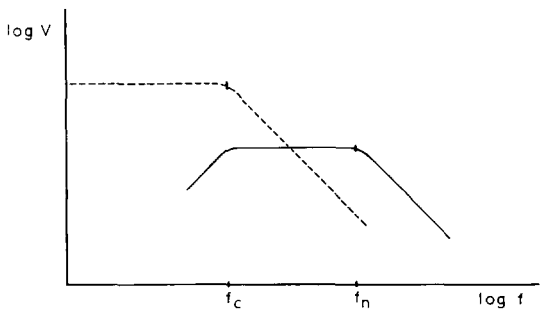


Fig. 10. Schematic diagram of the frequency dependence (according to Eqns. 7 and 10) of the induced potential across the plasmalemma (upper curve) and across the nuclear membrane (lower curve) for a constant external field strength, $E$; $f_c$ is the cut-off frequency of the plasmalemma and $f_n$ the cut-off frequency of the nuclear membrane.

sumption seems to be reasonable in the light of the experimental evidence given above if cells of approximately equal size and physiological state were used. For $P < 1$, $F_2$ is, therefore, equal to $P$ and $F_3$ is equal to $P \cdot P$ if for each contact region the same fusion probability exists. Correspondingly, the fusion index of $n$ cells in long chains is given by:

$$F_n = P^{n-1} \tag{6}$$

The excellent agreement between the prediction of Eqn. 6 and the experimental results gives strong support for the assumption of constant fusion probability along a cell chain which is $P = 0.4$ for V 79-EAT and $P = 0.35$ for Muntjac-EAT according to Fig. 9. Taking into account the probability value of $P < 0.5$ it is immediately obvious that linear fusion of more than six cells is a rather unlikely event ($F_6 = P^5 = 0.01 = 1\%$) at low suspension density. Since in each experiment about $1 \cdot 10^7$ cells were subjected to electrofusion Eqn. 4 predicts the occurrence of about five separate chains formed by linear fusion of 20 cells. This prediction is in reasonable agreement with the experimental finding. Towards higher suspension densities the formation of adjacent cell chains increased, resulting in the fusion of cells between different chains, with the consequence that Eqn. 6 is no longer valid.

## Discussion

Nuclear membrane fusion is a frequent event in electrofused cells, at least in conductive fusion media. This is in contrast to chemically or virally induced fusion. Cell synchronisation is obviously not a necessary pre-requisite for the fusion of nuclei if cell fusion is mediated by electric field treatment. The data presented here suggest that the alignment field induced a movement of the nuclei into the contact region of two adjacent cells. This caused the probability of nuclei fusion to be significantly increased once cytoplasmic continuum between two cells had been established in response to the breakdown pulse. Intracellular dielectrophoresis [20] in the frequency range used here requires that a potential difference be built up across the nuclear membrane within the intact cell. Theory [18,21] shows that as the frequency of an alternating field increases significantly, the plasmalemma capacity no longer shields the cell interior from participation in the conduction process. In this case the more general expression for the generated membrane voltage is:

$$V = \frac{1.5 \cdot a \cdot E \cdot \cos \nu}{\sqrt{(1 + (2\pi f \tau)^2)}} \tag{7}$$

whereby $f$ = the frequency of the alternating field and $\tau$ = the time constant of the $\beta$ dispersion given by:

$$\frac{1}{\tau} = \frac{1}{R_m \cdot C_m} + \frac{1}{a \cdot C_m (\rho_i + 0.5\rho_e)} \tag{8}$$

$R_m$ = specific membrane resistance, $C_m$ = specific membrane capacitance, $\rho_i$ and $\rho_e$ the specific internal and external resistivities, respectively.

If the $R_m C_m$ term in Eqn. 8 can be neglected in relation to the 'conductivity' term Eqn. 8 can be rewritten as:

$$\tau = a \cdot C_m (\rho_i + 0.5\rho_e) \tag{9}$$

This approximation is fulfilled for a typical cell surrounded by electrolyte solution which exhibits a specific membrane resistance of the order of 1 k$\Omega \cdot$ cm. For nuclear membranes, however, the $RC$ term may be of the order of the conductivity term, because of the relatively low specific membrane

resistance, $R_m$, of the nuclear membrane. Löwenstein and Kanno [22] measured a value of about 1 $\Omega \cdot$ cm in isolated nuclei of gland cells of *Drosophila flavorepleta* and a variety of oocytes with nuclei large enough to be measured with microelectrodes.

When $f \ll 1/2\pi\tau$ Eqn. 7 (in combination with Eqn. 9) reduces to Eqn. 10:

$$V = \frac{1.5 \cdot E \cdot \cos \nu}{2\pi f \cdot C_m \cdot (\rho_i + 0.5\rho_e)} \tag{10}$$

At high frequencies ($f \gg 1/2\ \pi\tau$) the membrane potential is independent of the radius of the cell, but is inversely proportional to the frequency. Fig. 10 schematically represents the frequency dependence of the membrane potential difference in response to an alternating field of constant amplitude. The 'cut-off' frequency is equal to $1/2\pi\tau$. Below the cellular cut-off frequency the nucleus is shielded by the plasmalemma and therefore its membrane potential increases linearly with frequency above a certain frequency (just below the $\beta$ dispersion [18]) until the cellular cut-off frequency is reached as shown schematically in Fig. 10. Towards higher frequencies the nuclear membrane potential remains constant. When the cut-off frequency of the nuclear membrane is reached, the nuclear membrane receives a potential equal to that of the cellular membrane at higher frequencies. As also show in Fig. 10 the nuclear membrane potential is always lower than that of the plasmalemma potential because of the smaller radius of the nucleus. Clearly, the charging time constant of the nuclear membrane is shorter (see Eqn. 7) than that of the cell membrane.

These considerations explain why the maximum values of both the cell and nuclear membrane fusion indices were observed between 1 and 4 MHz (depending on cell and nucleus size of the particular species). Specifically, the cellular cut-off frequency of the cells is about 1 MHz if we assume that the specific membrane capacitance is 1 $\mu$F/cm$^2$, the radius 10 $\mu$m and the specific resistivities $\rho_e = \rho_i = 100\ \Omega \cdot$ cm. Only above this frequency can intracellular dielectrophoresis of the nuclei occur. Towards higher frequencies both fusion indices must decrease because of the decrease in both cellular and nuclear membrane potential differences. It is obvious that the membrane potential difference has to exceed a certain value in order to induce vectorial displacement of the nuclei.

The explanation given above for the experimental findings implies that a sufficient membrane potential difference can be built up across the nuclear membrane in the frequency range in which the nuclear membrane index assumed its maximum value. This means that the membrane is not too conductive. Preliminary experiments with mechanically isolated nuclei from hepatocytes (Broda and Zimmermann, unpublished data) showed that nuclei exhibit dielectrophoresis leading to chain formation. Breakdown experiments using a hydrodynamically focussing particle analyser also showed that breakdown of the nuclear membrane can be induced. Breakdown occurred at a field strength in the orifice corresponding to a breakdown voltage of the nuclear membrane of 2 V. This value of the breakdown voltage of the nuclear membrane seems to be reasonable in the light of a breakdown voltage of a unit membrane of 1 V [1–5] because of the double layer structure of the nuclear membrane. This experimental finding is supported by theory which requires reconsideration of Eqn. 5 used for the calculation of the membrane potential generated by a field pulse (at low frequency). Jeltsch and Zimmermann [17] have shown that Eqn. 5 is an approximation to the following Eqn. 11 for the case of a low specific membrane resistance:

$$V = 1.5 \cdot a \cdot E \cdot \frac{1}{1+\lambda} \cdot \cos \nu \tag{11}$$

which is derived from the exact solution of the Laplace equation. The term, $\lambda$, is given by:

$$\lambda = \frac{\sigma_m}{d} \cdot a(\rho_i + 0.5\rho_e) \tag{12}$$

with $\sigma_m$ = specific membrane conductance and $d$ = thickness of membrane.

Introduction of the values of the specific membrane resistance and of the specific internal nuclear and cytoplasmic resistivities $\rho_i$ and $\rho_e$ (assuming both to be 100 $\Omega \cdot$ cm) yields a value of about 0.15 for $\lambda$. This value only leads to a reduction of the generated potential across the nuclear membrane by about 10% calculated according to Eqn. 5.

Thus, we can safely conclude that a sufficient membrane potential is generated across the nuclear membrane in the frequency range in which the plasmalemma impedance becomes negligible. Consequently, the observed movement of the nuclei into the contact zone resulted from intracellular dielectrophoresis. Movement of the nuclei occur in the direction of the contact zone due to dipole-dipole interaction between the two nuclei and due to the constriction of the field lines in the contact zone (see Fig. 20 in Ref. 4).

This physically-induced repositioning of the nuclei may have been one of the main reasons why electrofusion led to very high yields of hybrids if the frequency of the alignment field was around 1 MHz (see also Ref. 23). In addition, the experiments and theoretical considerations presented here may pave the way for further improvement of electrofusion of various cell types because it is obvious that the yield of hybrids should be correlated to the extent of nuclear membrane fusion.

Another aspect of the results presented here is the enhancing effect of externally added ATP on the fusion indices of ATP-depleted cells taken from an unfed plateau-phase. This finding is consistent with observations of Verhoek-Köhler et al. [24]. These authors studied the effect of ATP content on the fusion kinetics of mesophyll protoplasts of *Avena sativa* in the presence of inhibitors of photosynthesis. In these experiments a low ATP content either considerably delayed or even prevented the rounding-up time of the fusion product. Verhoek-Köhler et al. [24] suggested that the ATP level may influence membrane fluidity and, in turn, the lateral diffusion and randomisation of the individual lipid and protein molecules of the parental cells during the fusion process. Indeed, further experiments are required to reveal the complete potential of the effect of energy state on hybrid yield. It is quite conceivable that addition of GTP, which is known to stimulate fusion of membranes of isolated nuclei [7], or addition of other compounds may lead to a further increase in hybrid yields in special cell systems.

The experimental proof that fusion in long chains of aligned cells is apparently controlled by the probability of the two-cell fusion event is a further result worthy of discussion. The constant probability may explain why a large yield of hybrids is obtained from relatively high cell suspension densities irrespective of the procedure used for the establishment of a close membrane contact (e.g. by ultrasound [25], by magnetic fields [26] or by use of very high suspension densities [27]). This inherent feature of electrofusion is obviously the second reason why this physical technique is demonstrably superior to the conventional techniques (which are based on random fusion) and also paves the way for the development of efficient protocols for fusion of other cell types (e.g. of myeloma cells with lymphocytes for the production of hybridoma cells secreting monoclonal antibodies).

The data presented here suggest that field conditions and media composition which lead to an optimum and constant probability for fusion between two adhered cells, combined with optimum repositioning of the nuclei, must be developed.

## Acknowledgements

This work was supported by grants (EC-contract No. BI6-153-D) to U.B. and (SFB 176) to U.Z. Many thanks are due to Prof. Dr. W. Pohlit, Dr. M. Nüsse and the scientific staff of the Biophysikalische Strahlenforschung (Frankfurt) and Lehrstuhl für Biotechnology (Würzburg) for help in experimental work and for interesting discussions.

## References

1 Zimmermann, U., Scheurich, P., Pilwat, G. and Benz, R. (1981) Angew. Chem. (Int. Edn.) 20, 325–344.
2 Zimmermann, U. (1982) Biochim. Biophys. Acta 694, 227–277.
3 Zimmermann, U., Vienken, J. and Pilwat, G. (1984) in Investigative Microtechniques in Medicine and Biology, Vol. 1 (Chajen, J. and Bitensky, L., eds.), pp. 89–167, Marcel Dekker, New York.
4 Zimmermann, U. (1986) Rev. Physiol. Biochem. Pharmacol. 105, 175–256.
5 Zimmermann, U. and Urnovitz, H. (1987) Methods Enzymol. 151, 194–221.
6 Aronson, J.F. (1973) J. Cell. Biol. 58, 126–134.
7 Paiement, J. (1984) Biochim. Biophys. Acta 777, 274–282.
8 Zimmermann, U., Vienken, J., Pilwat, G. and Arnold, W.M. (1984) in Cell Fusion: Ciba Foundation Symposium, Vol. 103 (Evered, R. and Whelan, J., eds.), pp. 60–85, Pitman, London.
9 Richter, H.-P., Scheurich, P. and Zimmermann, U. (1981) Dev. Growth Differ. 23, 479–486.

10 Zimmermann, U., Riemann, F. and Pilwat, G. (1986) Biochim. Biophys. Acta 436, 460–474.
11 Stopper, H., Zimmermann, U. and Wecker, E. (1985) Z. Naturforsch. 402c, 133–139.
12 Stopper, H., Jones, H. and Zimmermann, U. (1987) Biochim. Biophys. Acta 900, 38–44.
13 Schnettler, R., Zimmermann, U. and Emeis, C.C. (1984) FEMS Microbiol. Lett. 24, 81–85.
14 Schnettler, R. and Zimmermann, U. (1985) FEMS Microbiol. Lett. 27, 195–198.
15 Nüsse, M. and Egner, H.G. (1984) Cell Tissue Kinet. 127, 13–23.
16 Pilwat, G. and Zimmermann, U. (1985) Biochim. Biophys. Acta 820, 305–314.
17 Jeltsch, E. and Zimmermann, U. (1979) Bioelectrochem. Bioenerg. 76, 349–384.
18 Schwan, P. (1983) in Biological Effects and Dosimetry of nonionizing Radiation (Grandolfo, M., Michaelson, S.M. and Rindl, A., eds.), pp. 213–231, Plenum Publishing Corp., New York.
19 Rao, P.N., Wilson, B. and Puck, T.T. (1976) J. Cell Physiol. 91, 131–142.
20 Pethig, R. (1979) Dielectric and Electronic Properties of Biological Materials, John Wiley & Sons, Chichester, New York.
21 Holzapfel, C., Vienken, J. and Zimmermann, U. (1982) J. Membr. Biol. 67, 13–26.
22 Löwenstein, W.R. and Kanno, Y. (1963) J. Gen. Physiol. 46, 1123–1140.
23 Stoy, R.D., Forster, K.R. and Schwan, P. (1982) Phys. Med. Biol. 27, 501–513.
24 Verhoek-Köhler, B., Hampp, R., Ziegler, H. and Zimmermann, U. (1983) Planta 159, 199–204.
25 Vienken, J., Zimmermann, U., Zenner, H.P., Coakley, W.T. and Gould, R.K. (1985) Biochim. Biophys. Acta 820, 259–264.
26 Kramer, I., Vienken, K., Vienken, J. and Zimmermann, U. (1984) Biochim. Biophys. Acta 772, 407–410.
27 Zimmermann, U., Vienken, J., Halfmann, J. and Emeis, C.C. (1985) in Advances in Biotechnological Processes, Vol. 4 (Mizrahi, A. and Van Wezel, A.L., eds.), pp. 79–151, Alan R. Liss, New York.